



# The effect of organic nucleation on the indirect radiative forcing with a semi-explicit chemical mechanism for highly oxygenated organic molecules (HOMs)

5 Xinyue Shao<sup>1,2</sup>, Minghuai Wang<sup>1,2</sup>, Xinyi Dong<sup>1,2,3</sup>, Yaman Liu<sup>1,4</sup>, Stephen R. Arnold<sup>5</sup>, Leighton A. Regayre<sup>5,6,7</sup>, Duseong S. Jo<sup>8</sup>, Wenxiang Shen<sup>1,2</sup>, Hao Wang<sup>1,2</sup>, Man Yue<sup>1,4</sup>, Jingyi Wang<sup>1,2</sup>, Wenxin Zhang<sup>1,2</sup>, and Ken S. Carslaw<sup>5</sup>

<sup>1</sup>School of Atmospheric Science, Nanjing University, Nanjing, 210023, China

10 <sup>2</sup>Joint International Research Laboratory of Atmospheric and Earth System Sciences & Institute for Climate and Global Change Research, Nanjing University, Nanjing, 210023, China

<sup>3</sup>Frontiers Science Center for Critical Earth Material Cycling, Nanjing University, Nanjing, China

<sup>4</sup>Zhejiang Institute of Meteorological Sciences, Hangzhou, 310008, China

<sup>5</sup>School of Earth and Environment, University of Leeds, Leeds, LS2 9JT, UK

15 <sup>6</sup>Met Office Hadley Centre, Exeter, Fitzroy Road, Exeter, Devon, EX1 3PB, UK

<sup>7</sup>Centre for Environmental Modelling and Computation, School of Earth and Environment, University of Leeds, Leeds, LS2 9JT, UK

<sup>8</sup>Department of Earth Science Education, Seoul National University, Seoul, 08826, South Korea

*Correspondence to:* Minghuai Wang ([minghuai.wang@nju.edu.cn](mailto:minghuai.wang@nju.edu.cn)), Xinyi Dong ([dongxy@nju.edu.cn](mailto:dongxy@nju.edu.cn))

20 **Abstract.** Highly oxygenated organic molecules (HOMs) can significantly contribute to new particle formation (NPF). HOMs-derived NPF in preindustrial (PI) environments provides the baseline for calculating radiative forcing, yet global model studies examining this are lacking. Here, we use a global climate model with a semi-explicit HOMs chemistry and the associated nucleation scheme to systematically quantify the effect of HOMs-derived NPF on CCN formation and effective radiative forcing due to aerosol–cloud interactions (ERF<sub>aci</sub>). The model shows better agreement with measured cloud condensation  
25 nuclei (CCN) numbers after including organic NPF mechanisms. Aerosols generated from organic NPF nearly double the globally averaged CCN burden in PI (39%) compared to PD (18%) experiments. This weakens the ERF<sub>aci</sub> by 0.4 W m<sup>-2</sup>, corresponding to a 16% reduction, with most of this reduction occurring in tropical regions where the pure organic nucleation rate shows larger value in PI atmosphere. Unlike the findings of Gordon et al. (2016), the reduction is mainly driven by a  
30 greater enhancement of the sub-20 nm growth rate (GR) in the PI atmosphere compared to PD instead of the ~1 nm nucleation rate ( $j_{1.7\text{nm}}$ ). The greater enhancement of GR is due to higher HOM concentrations in the PI atmosphere, while the greater  $j_{1.7\text{nm}}$  in PD environment results from higher sulfuric acid concentrations, leading to higher heteromolecular nucleation rates involving sulfuric acid and organics. The significant reduction underscores the critical role of biogenic NPF in CCN formation, particularly in the PI climate when cloud droplet concentrations and albedo are more sensitive to aerosol changes.



## 1 Introduction

35 Atmospheric aerosols can affect climate indirectly by acting as cloud condensation nuclei (CCN), which modify cloud  
properties and precipitation (Rosenfeld and Lensky, 1998; Rosenfeld and Woodley, 2000; Twomey, 1977; Albrecht, 1989).  
The effective radiative forcing due to aerosol–cloud interactions ( $ERF_{aci}$ ) remains one of the largest uncertainties in interpreting  
40 climate change over the past century and projecting future changes (Watson-Parris and Smith, 2022; Peace et al., 2020).  
Atmospheric new particle formation (NPF) is the largest source of atmospheric aerosol number concentrations (Gordon et al.,  
2017; Lee et al., 2019) and is thought to contribute up to half of the global cloud condensation nuclei (CCN) number (Spracklen  
et al., 2008; Merikanto et al., 2009; Williamson et al., 2019). Global climate model simulations indicate that aerosol  $ERF_{aci}$  is  
sensitive to parameterizations of NPF processes (Wang and Penner, 2009; Kazil et al., 2010; Gordon et al., 2017; Zhu et al.,  
2019; Yu et al., 2012).

45 Recent studies have highlighted the significant role of monoterpene-derived highly oxygenated organic molecules (HOMs) in  
NPF processes and their potential impact on regulating CCN concentrations, even in the absence of sulfuric acid. Ehn et al.  
(2014) found significant contributions of HOMs to the growth of particles ranging from 5 to 50 nm in diameter in boreal forests.  
Jokinen et al. (2015) showed that monoterpene-derived HOMs facilitate new particle formation and growth in continental  
50 regions, especially under conditions of high supersaturation, favorably affecting the concentration of CCN using chamber  
experiments. Using the regional model WRF-Chem, Zhao et al. (2020) showed that in the Amazon region biogenic HOMs  
predominantly lead to the formation of new particles at altitudes of 13 km, in a location minimally influenced by human  
activities, thereby making a significant contribution to CCN formation (Zhao et al., 2022). Similarly, Wang et al. (2023)  
analyzed the sources of aerosols in the Amazonian boundary layer using the HadGEM3 climate model incorporating the  
biogenic nucleation mechanism along with its precursor gas (HOMs) from the parameterization in Gordon et al. (2016).

55 Although HOMs are important for NPF due to their low volatility, their chemical formation pathways remain uncertain, and  
are they treated in various simplified ways in models. Gordon et al. (2016) simulated monoterpene-derived HOMs formation  
using a fixed yield of HOMs from first-stage monoterpene oxidation products. Zhu et al. (2019) added some explicit chemical  
mechanisms for HOMs, but they did not consider autoxidation and used a less stringent definition of HOMs than recommended  
60 in Bianchi et al. (2019). Also, they did not account for organic nucleating species oxidized from isoprene. Therefore, the  
contribution of accretion products (ACCs) generated from cross-reactions of isoprene- and monoterpene-derived radicals was  
significantly underestimated. Roldin et al. (2019) and Weber et al. (2020) employed a more explicit reaction mechanisms to  
treat the generation of HOMs through autoxidation and cross-reactions of  $\alpha$ -pinene oxidation products, but neither applied  
these chemical mechanisms on a global scale. Xu et al. (2022) summarized various chemical mechanisms of HOMs, including  
65 monoterpene-derived peroxy radical (MT-RO<sub>2</sub>) unimolecular autoxidation and self- and cross-reactions with other RO<sub>2</sub> species  
in the GEOS-Chem global model but did not consider their role in the NPF process.



70 HOM-driven NPF is likely to be particularly important in the pristine preindustrial (PI) atmosphere, where concentrations of  
sulfuric acid and ammonia were much lower. Simulations of the pre-industrial atmosphere form the baseline for calculations  
of anthropogenic radiative forcing in global models (Carslaw et al., 2013). Using global model simulations, Gordon et al.  
(2016) showed that new particles formed from monoterpene-derived HOMs could increase CCN concentrations in the PI  
environment by 20% to 100%. This increase led to a 27% reduction in negative radiative forcing due to changes in cloud  
albedo since 1750, decreasing by between  $-0.28 \text{ W m}^{-2}$  and  $-0.06 \text{ W m}^{-2}$ . Similarly, Zhu et al. (2019), utilizing simulations  
75 with the Community Earth System Model (CESM), found that new particles formed from monoterpene-derived HOMs have  
reduced the direct plus indirect radiative forcing of aerosols by 12.5% since the Industrial Revolution. However, they did not  
use explicit chemical processes to represent HOMs chemistry, potentially leading to inaccuracies in the PI and present-day  
(PD) simulations for radiative forcing calculations due to anthropogenic emissions. The uncertainty in this baseline is one of  
the largest components of the overall uncertainty in aerosol radiative forcing (Seinfeld et al., 2016; Carslaw et al., 2013).

80 Considering the unequivocal evidence for the role of biogenic organics in producing atmospheric particles, we have recently  
incorporated a state-of-the-art representation of HOMs from various chamber experiments (Xu et al., 2022b) and update the  
nucleation scheme involving HOMs, ACCs,  $\text{H}_2\text{SO}_4$ ,  $\text{NH}_3$ , and ions from previously published CLOUD chamber experiments  
in a global chemistry-climate model (Shao et al., 2024). Additionally, Shao et al. (2024) account for organics condensing on  
newly formed sub-20 nm particles. The updated model demonstrates significant improvements in simulating NPF events and  
85 aerosol number concentrations, showing better agreement with measurements (Shao et al., 2024). Here, we seek to estimate  
the change in  $\text{ERF}_{\text{aci}}$  resulting from the inclusion of organic particle formation based on this model, and highlight the key  
processes driving this change.

The model and field measurements used in this study are documented in Section 2. Section 3 evaluates CCN number  
90 concentrations in the updated model. Section 4 quantifies the contributions of organic NPF to CCN number globally in both  
present day (PD) and PI environments. The change in effective radiative forcing due to aerosol–cloud interactions ( $\text{ERF}_{\text{aci}}$ )  
associated with organic NPF processes is also calculated. Results are summarized and discussed in Section 5.

## 95 **2 Data and methods**

### **2.1 Model configuration**

In this study, we examine the impact of organic NPF on atmospheric aerosols and the Earth's radiative balance using the  
atmospheric module of the Community Earth System Model (CESM) version 2.1.0, specifically the Community Atmosphere  
Model version 6, which is enhanced with extensive tropospheric and stratospheric chemistry (CAM6-Chem) (Emmons et al.,  
100 2020). The model uses the MOZART-TS2 gas-phase chemistry scheme (Schwantes et al., 2020) and employs a four-mode



version of the Modal Aerosol Module (MAM4) (Liu et al., 2016). The default configuration of CAM6-Chem includes binary homogeneous nucleation of  $\text{H}_2\text{SO}_4\text{-H}_2\text{O}$  (Vehkamaki et al., 2002) and ternary homogeneous nucleation of  $\text{H}_2\text{SO}_4\text{-NH}_3\text{-H}_2\text{O}$  (Merikanto et al., 2007). Additionally, within the boundary layer, the model includes the empirical nucleation mechanism (Kulmala et al., 2006; Sihto et al., 2006).

105

Our previous study (Shao et al., 2024) incorporated the representation of HOMs chemistry from Xu et al. (2022a) (including monoterpene derived peroxy radical (MT-RO<sub>2</sub>) unimolecular autoxidation and self- and cross-reactions with other RO<sub>2</sub> species). In total, 24 reactions in CAM6-Chem were modified and 96 reactions were added to more explicitly simulated HOMs chemistry (Section S1). Shao et al. (2024) also updated inorganic nucleation rates involving  $\text{H}_2\text{SO}_4$  and  $\text{NH}_3$  as well as ion-induced pathways based on the CLOUD chamber experiments (Dunne et al., 2016), replacing the default scheme based on  $\text{H}_2\text{SO}_4$  and  $\text{NH}_3$  (Vehkamaki et al., 2002; Merikanto et al., 2007). The organic nucleation scheme was also added in CAM6-Chem, including heteromolecular nucleation of sulfuric acid and organics ( $J_{\text{SA-Org}}$ ) (Riccobono et al., 2014), neutral pure organic nucleation ( $J_{\text{Org,n}}$ ) and ion-induced pure organic nucleation ( $J_{\text{Org,i}}$ ) (Kirkby et al., 2016). Organic vapor condensation on newly formed particles was also added in our updated model (Eq. (12) in Shao et al. (2024)).

115

All the above mentioned updated nucleation rate and sub-20 nm particle growth rates have already been evaluated in our previous study (Shao et al., 2024), in better agreement with observations at numerous sites. Therefore, the performance of NPF event frequency and N10 (number concentrations for particles with diameters larger than 10 nm) also shows reasonable agreement with measurements (Shao et al., 2024).

120

## 2.2 Case setting

We calculated the  $\text{ERF}_{\text{aci}}$  between preindustrial (PI) and present-day (PD) using the methodology from Ghan (2013). The effect of biogenic organic NPF on the magnitude of  $\text{ERF}_{\text{aci}}$  was calculated by comparing simulations with (using Eq. (2)-(8) in Shao et al. (2024), named “Inorg\_Org” in table 1) and without (only using Eq. (6)-(8) in Shao et al. (2024), named “Inorg” in table 1) biogenic NPF mechanisms. The prefixes “PD” and “PI” in each test name represent emissions scenarios appropriate to present day and preindustrial (Table 1).

125

Ten-year simulations were performed with  $0.9^\circ \times 1.25^\circ$  spatial resolution and a vertical resolution extending up to approximately 40 km across 32 layers (Emmons et al., 2020) for both present-day (PD) and preindustrial (PI) atmospheres with an additional one-year spin-up period (Table 1). Sea surface temperature and sea-ice extents are prescribed to climatological values for the year 2000 in both PD and PI cases. Anthropogenic and monthly biomass burning emissions are provided by the Community Emission Data System (CEDS v2017-05-18) (Hoesly et al., 2018) and the historical global biomass burning emissions inventory (van Marle et al., 2017) developed for CMIP6. For PD simulation, emissions after 2014 follow the SSP585 scenario, based on the Shared Socioeconomic Pathway 5 (SSP5) (O'Neill et al., 2017). Biogenic emissions

130



135 are dynamically simulated using the Model of Emissions of Gases and Aerosol from Nature version 2.1 (MEGAN2.1) (Guenther et al., 2012). The Multi-resolution Emission Inventory for China (MEIC) (<http://www.meicmodel.org>) (Li et al., 2017; Yue et al., 2023) was used to replace the CMIP6 emission inventory for China, as CMIP6 underestimates the reduction of SO<sub>2</sub> emissions after 2007.

140 In order to compare simulated CCN with measurements, several short-term simulations were performed, in which meteorological fields (temperature and wind profiles, surface pressure, surface stress, surface heat and moisture fluxes) were nudged toward Modern-Era Retrospective analysis for Research and Applications (MERRA2) reanalysis (Koopman et al., 2012). The simulation period corresponded to the time of measurements (Table 2), with an additional month for spin-up.

145 **Table 1.** Configurations of CESM2.1.0 Experiments (long-term simulation)

Test Name	Simulation period	Spin-up	Updated inorganic nucleation	HOMs chemistry	Organic nucleation and growth
Inorg	corresponds to the measurements in Table 2	one month	✓	✓	×
Inorg_Org			✓	✓	✓
PD_Inorg	2008.1-2017.12	one year (2007.1-2007.12)	✓	✓	×
PD_Inorg_Org			✓	✓	✓
PI_Inorg	1851.1-1860.12	one year (1850.1-1850.12)	✓	✓	×
PI_Inorg_Org			✓	✓	✓

### 2.3 Observation data

150 In our previous study (Shao et al., 2024), we evaluated NPF-related variables, including nucleation rate, growth rate, NPF frequency, condensation sink, and aerosol number concentration in the updated model. Here, we focus specifically on evaluating the CCN number concentration in both Inorg\_Org and Inorg models. The CCN number concentration is crucial because it influences the degree of cooling of the Earth's surface through the aerosol-cloud interaction, specifically by influencing cloud albedo and cloud lifetime (Twomey, 1977; Albrecht, 1989).

155 The observational data of CCN number concentrations used in this study were obtained from ships, stations, and aircraft at various locations (see Table 2) (Jefferson, 2010; Uin et al., 2019; Bodhaine, 1983; Wang et al., 2022; Wood et al., 2015; Zheng



et al., 2020) (all the data are available for download at <http://www.archive.arm.gov/discovery/#v/results/>). All data were processed within the Global Aerosol Synthesis and Science Project (GASSP) (Reddington et al., 2017). The CCN number measurements exhibit a very high temporal resolution (<1 minute). However, the model output's physical time step is only half an hour, making it impossible to precisely match the observation data with the model output. Consequently, we selected CCN number concentrations at supersaturations (ss) of 0.1%, 0.2%, 0.5%, and 1% from the observational data to represent different atmospheric supersaturations. These values were then compared with the model's monthly average output at the same supersaturation levels for the corresponding time period (Fig. 1).

165

**Table 2.** Field measurements used in this study

Station	Type	Altitude (m asl)	Latitude	Longitude	Time
Barrow, Alaska, USA	Marine	8.0	71.32° N	156.61° W	2008/01-2013/01
Eastern North Atlantic	Marine	26.0	39.09° N	28.03° W	2014/11-2015-04
Graciosa Island	Marine	26.0	39.09° N	28.03° W	2009/05-2010/11
Manacapuru, Brazil	Urban	50.0	-3.21° S	60.60° W	2014/02-2015/05
Nainital, India	Mountain	1936.0	29.36° N	79.46° E	2011/06-2012/03
Shouxian, China	Rural	22.7	32.56° N	116.78° E	2008/05-2008/10
Steamboat Springs, USA	Mountain	2440.0	40.45° N	106.79° W	2010/10-2011/04
Chilbolton, UK	Rural	80.0	51.15° N	1.44° W	2009/02-03

### 3 Evaluation of simulated CCN concentrations

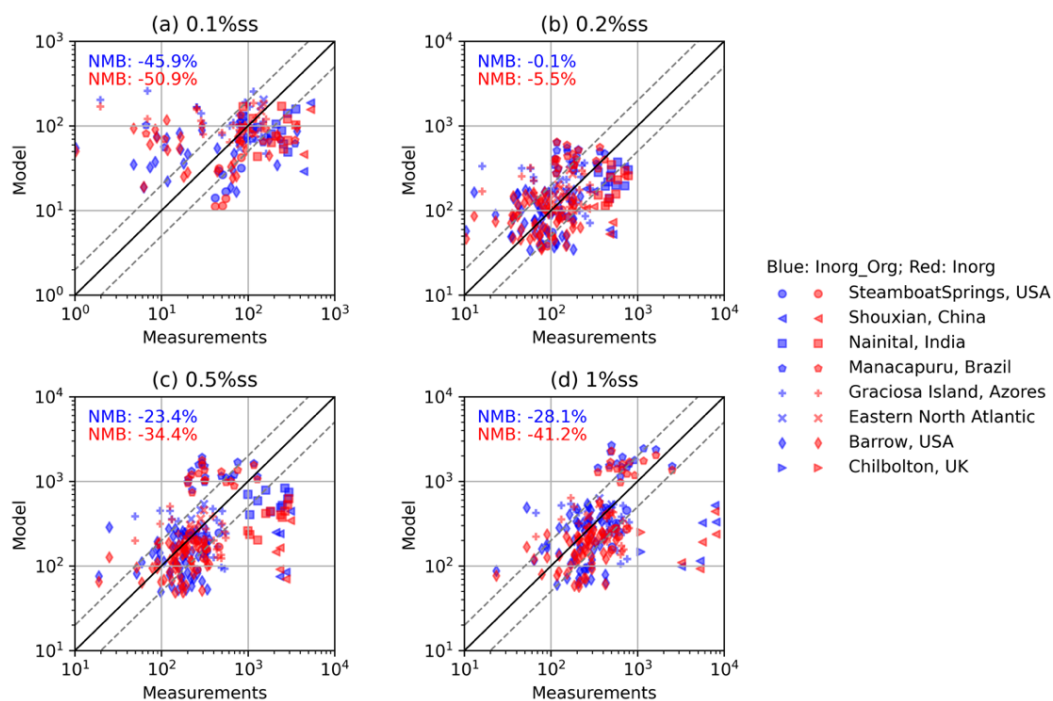
CCN number concentrations in the Inorg\_Org model at 0.1%, 0.2%, 0.5%, and 1% supersaturation (ss) show better agreement with measurements from various locations compared to the Inorg model (Fig. 1). The underestimation of CCN numbers in the Inorg simulation is alleviated by incorporating organic-related NPF, especially over rural and mountainous regions such as Steamboat Springs, Shouxian, and Nainital (Fig. 1), where both nucleation and initial growth rates are dominated by biogenic pathways. However, there remains a slight underestimation of CCN number in Shouxian at all supersaturation levels. This is likely due to the neglect of anthropogenic-derived HOMs to nucleation and growth, which are key NPF mechanisms in rural regions of China. The increase in CCN number due to the addition of organic NPF mechanisms is simulated not only in the locations listed in Table 1 but also on a global scale (see Fig. 7). "In urban regions of Brazil (Manacapuru), the overestimation of CCN numbers at 0.5% and 1% ss in Inorg is exacerbated (Fig. 1). Apart from urban regions like Manacapuru, Brazil, the overestimation also increases over oceanic regions such as Barrow and Graciosa. These overestimations in CCN numbers in the Inorg model are likely related to the overestimation of H<sub>2</sub>SO<sub>4</sub> concentration in CAM6-Chem (Shao et al., 2024). Overall,

170

175



180 the normalized mean bias (NMB) of CCN numbers at different supersaturation levels decreases from -35% (Inorg) to -24% (Inorg\_Org), indicating that the Inorg\_Org model provides a more accurate representation of organic contributions for further quantification in Section 3.



185 **Figure 1.** Comparison of simulated (monthly mean) and measured CCN number (median value) concentration (unit:  $\text{cm}^{-3}$ ) at (a) 0.1% supersaturation (ss), (b) 0.2% ss, (c) 0.5%ss, and (d) 1% ss in Inorg\_Org (blue symbols) and Inorg (red symbols). Information regarding the measurement sites is summarized in **Table 2**. Normalized mean bias (NMB) values are shown on the top left of each figure.

## 190 4 Results

### 4.1 Change in CCN and cloud droplet number concentrations

The inclusion of organic NPF results in a greater increase in the CCN burden in the PI experiment ( $\sim 39\%$ ) compared to the PD experiment ( $\sim 18\%$ ) (Fig. 2). The spatial pattern of change in CCN burden (Fig. 2) is consistent with the change in aerosol burden in the Aitken and accumulation mode (Figs. S11 and S12) but affects much wider areas because of the slower removal rate of larger aerosol particles. On the western side of the Amazon basin, the highest rise ( $>50\%$ ) in both the PD and PI experiments is caused by high CCN burden transported from the Amazon basin. Such a significant change in CCN production across the unpolluted PI atmosphere is particularly important for global climate because cloud droplet number concentrations (CDNC) are sensitive to CCN changes. Therefore, CDNC at the top of low clouds in Inorg\_Org rise by 12% in the PI experiments but only 7% in the PD experiments compared to Inorg (Fig. 3).

200



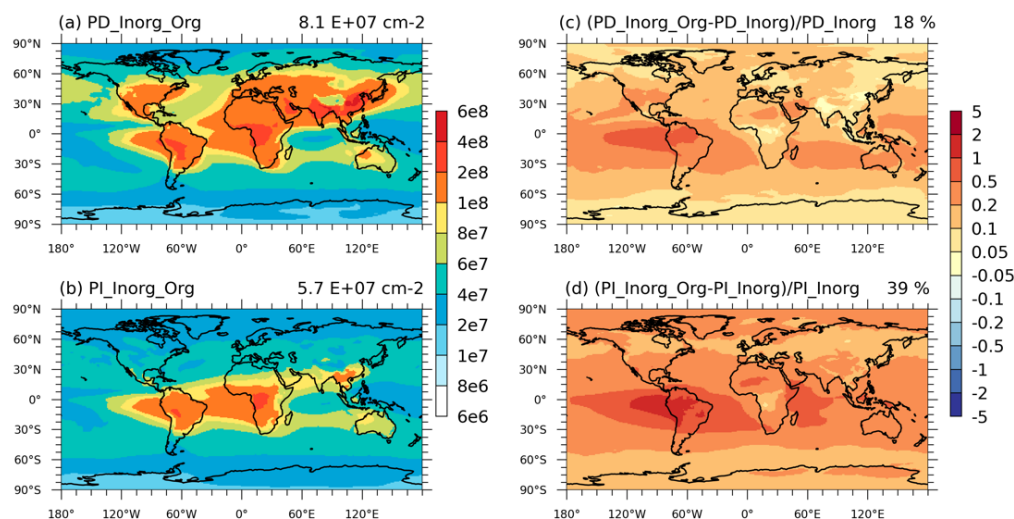


**Figure 2.** Spatial distribution of the simulated vertically-integrated CCN at 0.2% supersaturation (ss) in (a) PD\_Inorg\_Org and (b) PI\_Inorg\_Org (unit:  $\text{cm}^{-2}$ ). The relative change after adding organic NPF in PD and PI environments are shown in (c) and (d). Global mean values are shown on the top right of each figure.

205

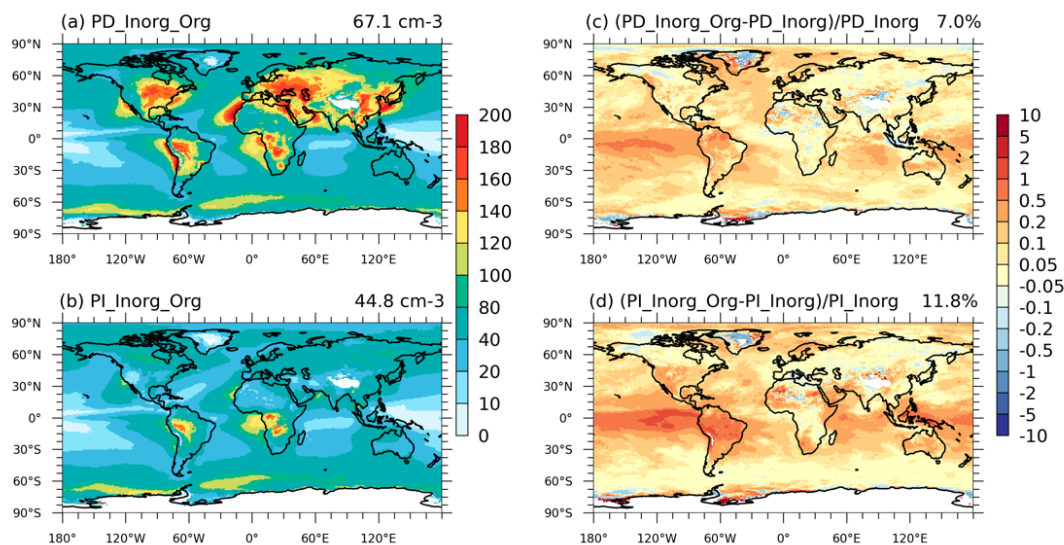


**Figure 3.** Spatial distribution of the simulated vertically-integrated cloud droplet number concentration (CDNC) at the top of low clouds in (a) PD\_Inorg\_Org and (b) PI\_Inorg\_Org (unit:  $\text{cm}^{-3}$ ). The relative change after adding organic NPF in PD and PI environments are shown in (c) and (d). Global mean values are shown on the top right of each figure.

210

In both PD and PI experiments, the largest increase in CCN burden ( $>20\%$  rise in Inorg\_Org compared to Inorg) is simulated in the tropical regions (Amazon, central Africa, and Southeast Asia) (Fig. 2). This is attributed to the highest biogenic emissions (Fig. S3) which lead to the greatest increases in both nucleation and growth rates in Inorg\_Org (Fig. 4) and a low aerosol number before adding organic NPF (i.e., Inorg simulation) in these regions. The enhancement in nucleation rates due to the

215





inclusion of organic nucleation is more significant in the PD experiment (39%) compared to the PI experiment (6%) (Fig. 4). This is mainly caused by higher sulfuric acid concentrations in PD environment (Fig. S2), resulting in higher heteromolecular nucleation rates involving sulfuric acid and organics (Figs. S6 and S7). A detailed discussion of the specific reason is provided in Section 4.2. Therefore, comparing to the increase in the  $\sim 1.7$  nm nucleation rate, the increase in the sub-20 nm growth rate plays a more significant role in greater increase of CCN burden in PI experiment (Fig. 4 and Fig. S13).

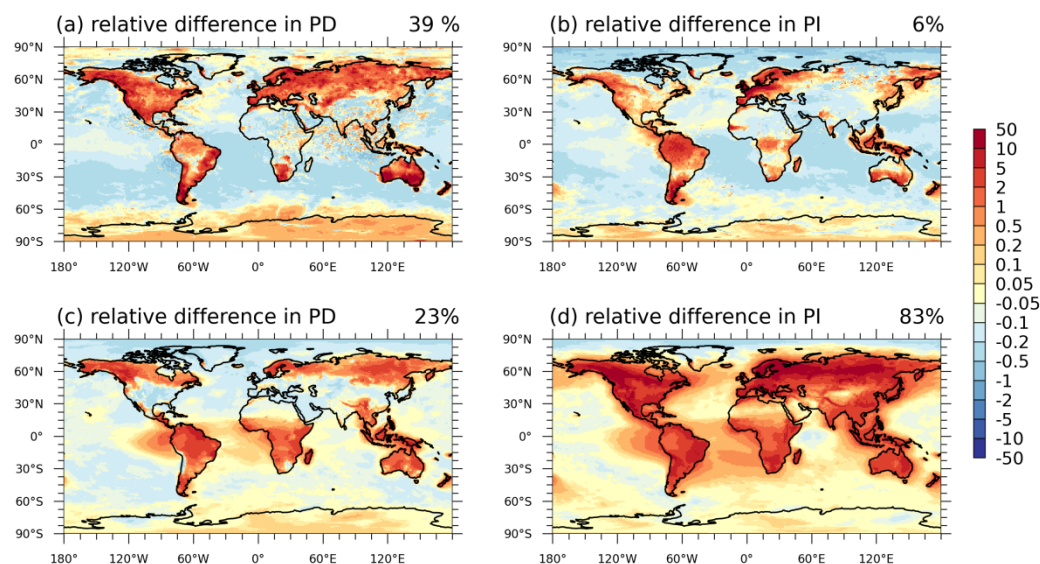
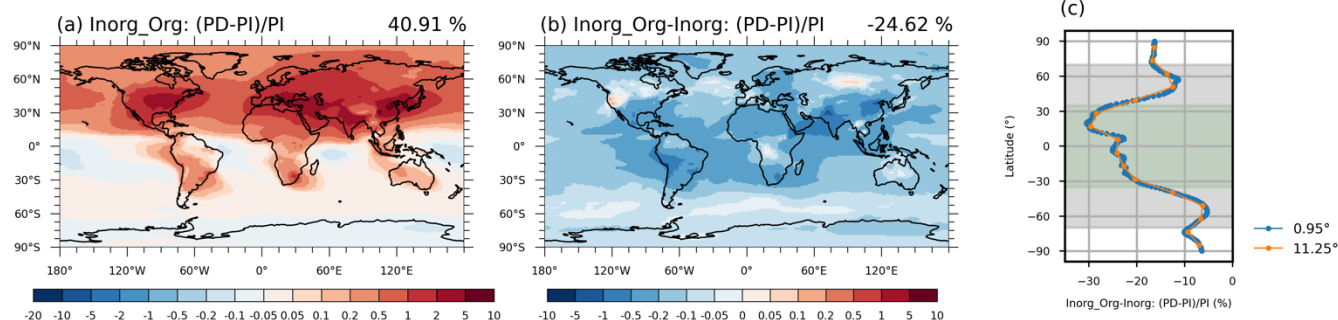


**Figure 4.** Spatial distribution in (a) PD\_Inorg\_Org and (b) PI\_Inorg\_Org (unit:  $\text{m}^{-2} \text{s}^{-1}$ ). The relative change of the simulated vertically-integrated nucleation rate ( $j_{1.7\text{nm}}$ , below 15 km) and vertically-mean sub-20nm growth rate after adding organic nucleation is shown in PD and PI environments. Global mean values are shown on the top right of each figure.

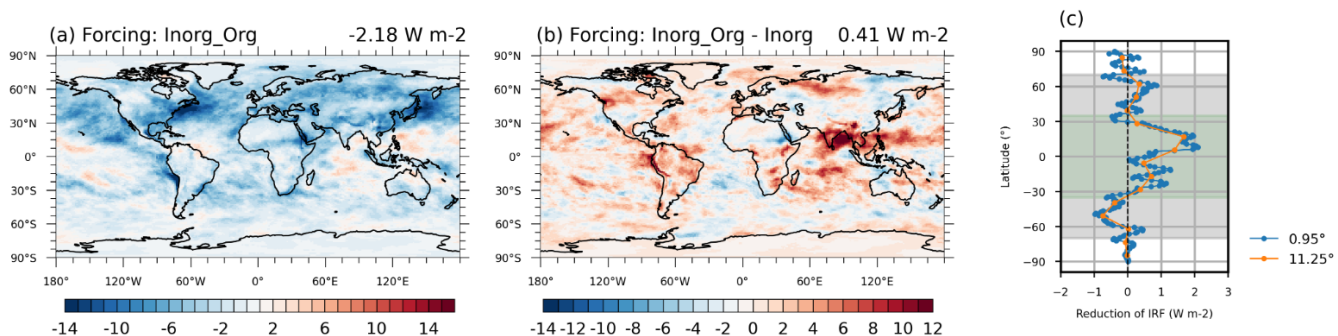
#### 4.2 Effect on aerosol indirect radiative forcing

The significant increase in CCN number and CDNC in the PI experiment resulting from the inclusion of the organic NPF scheme is likely to reduce the aerosol radiative forcing. The aerosol direct radiative forcing may not be significantly influenced by the NPF mechanism because it is not strongly affected by the aerosol size distribution (Rap et al., 2013). Thus, in this study we only quantify the effect of including biogenic organic NPF on the indirect aerosol forcing component ( $\text{ERF}_{\text{aci}}$ ). The effect of organic NPF on the magnitude of  $\text{ERF}_{\text{aci}}$  is calculated by comparing simulations with (Inorg\_Org) and without (Inorg) organic nucleation and growth mechanisms. To analyze the change in  $\text{ERF}_{\text{aci}}$ , we also compare the fractional changes of other key variables (nucleation rate, growth rate, aerosol number, CCN number, and CDNC) from PI to PD in Inorg\_Org and Inorg (Fig. 7).



240 **Figure 5.** The global mean of the relative change of vertically-integrated CCN number at 0.2% supersaturation in PD experiments compared  
to PI experiments after adding organic NPF mechanisms **(a)** and the difference of that value between with and without organic NPF **(b)**. The  
zonal mean of the information in **(b)** is shown in **(c)** (Blue scatters show the zonal mean with an interval of 0.95° and the orange scatters  
show the zonal mean with an interval of 11.25°). The global average value is shown on the top right of each panel. Model experiments are  
described in **Table 2** and model data come from monthly mean value over 10 years.

245



250 **Figure 6.** The effective radiative forcing due to aerosol–cloud interactions ( $ERF_{aci}$ ) aerosol after including organic NPF **(a)** and the difference  
in the  $ERF_{aci}$  of anthropogenic aerosol between with and without organic NPF **(b)**. The zonal mean of the information in **(b)** is shown in **(c)**  
(Blue scatters show the zonal mean with an interval of 0.95° and the orange scatters show the zonal mean with an interval of 11.25°). The  
global average value is shown on the top right of each panel. Model experiments are described in **Table 2** and model data come from monthly  
mean value over 10 years.

We estimate that the global  $ERF_{aci}$  since 1850, after including organic NPF, is  $-2.18 \text{ W m}^{-2}$  (Fig. 6a). The calculated aerosol  
255  $ERF_{aci}$  decreases by approximately  $0.4 \text{ W m}^{-2}$  (corresponding to a 16% reduction) after adding organic NPF mechanisms (Fig.  
6b). This reduction is attributed to the greater increase in CCN number in the PI experiment compared to the PD experiment  
(Fig. 2) when adding organic NPF (Inorg\_Org), leading to a smaller relative difference in these variables between the PD and  
PI experiments (66% in Inorg\_Org and 41% in Inorg, Fig. 7).

260 The largest reduction in  $ERF_{aci}$  occurs over the tropical region ( $-35^\circ$  to  $35^\circ \text{ N}$ ) (Fig. 6c), especially over oceans with high low  
cloud cover, such as the western side of the Amazon basin and eastern China (Fig. 6b). This corresponds to the change in the  
CCN number and CDNC in the PI experiments, which also shows the largest increase in tropical regions. The average  $ERF_{aci}$   
decreases by approximately  $1 \text{ W m}^{-2}$  between  $35^\circ \text{ S}$  and  $35^\circ \text{ N}$ , with a more significant effect in the Northern Hemisphere (NH)



(Fig. 6b and 6c). This is mainly attributed to the largest reduction in the PD fractional change of vertically-integrated CCN number in the northern United States, southeastern United States, and India in Inorg\_Org compared to Inorg (Fig. 5b). These significant reductions are transported to the western side of these regions, where most of the anthropogenic aerosol–cloud radiative forcing occurs, resulting in significant reductions in  $ERF_{aci}$  (Fig. 6b). The largest reduction of  $ERF_{aci}$  in the Southern Hemisphere (SH) occurs on the western side of the Amazon and Australia (Fig. 6b), where biogenic NPF causes the largest reduction in CCN concentrations from PD to PI experiment (Fig. 5a), driven by the large continental source of biogenic gases (Fig. S3). In some tropical oceanic regions of the SH, there are higher CCN concentrations in the PI atmosphere than PD in Inorg\_Org (Fig. 5a), caused by higher preindustrial ACCs (Fig. S3) and lower particle condensation sinks, leading to a positive  $ERF_{aci}$  (Fig. 5a). At mid-latitudes ( $35^{\circ}\sim 70^{\circ}$ ) in the NH, the reduction in  $ERF_{aci}$  is mainly caused by larger emissions of monoterpenes, and consequently, higher concentrations of HOMs in the PI environment of boreal forests in North America and Eurasia (Fig. S3). The large increase in sub-20 nm particle growth rate in the PI experiment resulting from HOM condensation also supports this point.

In previous studies (Zhu et al., 2019; Gordon et al., 2016), organic nucleation ( $J_{Org,n}+J_{Org,i}+J_{SA-Org}$ ) is the main reason for higher CCN number in PI simulation and thus leading to the reduction in  $ERF_{aci}$ . However, in our simulation, the fractional change in total nucleation rate from PI to PD is larger after adding organic nucleation (1075% in Inorg\_Org and 796% in Inorg) (Fig. 7). This is mainly caused by heteromolecular nucleation rate of sulfuric acid and organics rate ( $J_{SA-Org}$ ), which is the dominant contributor to total nucleation rate, showing greater increase in the PD experiment (Fig. S6) compared to PI experiment (Fig. S7). Especially in boreal forests, northern America, and Australia (Fig. S8), both  $H_2SO_4$  and HOMs are abundant in the PD experiments (Fig. S2 and S3), leading to much larger  $J_{SA-Org}$  values (Fig. S6). Therefore, the greater enhancement of CCN burden in PI experiment and reduction in  $ERF_{aci}$  are mainly caused by organic condensational growth on sub-20nm particles instead of organic nucleation.

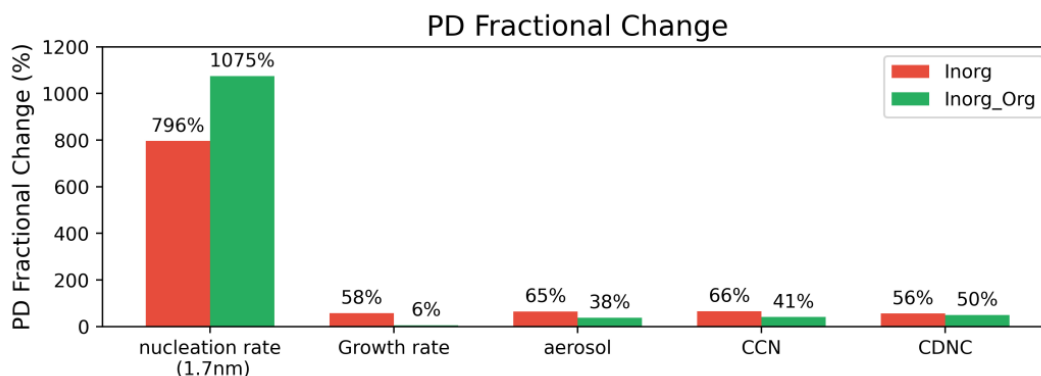


**Figure 7.** The global mean of the PD fractional change ((PD-PI)/PI) of key variables. Model experiments are described in Table 2 and model data come from monthly mean value over 10 years.



290

The most significant changes in  $ERF_{aci}$  reduction due to the inclusion of organic NPF are in tropical regions (Fig. 6c). This is different from previous studies (Zhu et al., 2019; Gordon et al., 2016), which showed that most of the reduction in  $ERF_{aci}$  occurs in the mid-latitudes of the NH, closely related to the distribution of HOM concentrations. Previous studies (Zhu et al., 2019; Gordon et al., 2016) did not account for organic nucleating species derived from isoprene oxidation, thereby neglecting ACC generation through self- and cross-reactions of isoprene- and monoterpene-derived radicals was neglected. Gordon et al. (2016) and Zhu et al. (2019) assumed that all organic nucleating species had the same volatility and can equally contribute to the organic nucleation. This simplification may have led to an overestimation of the organic nucleation rate and, consequently, the reduction in  $ERF_{aci}$  in the mid-latitudes. Our study highlights that only ACCs can contribute to pure organic nucleation due to their extremely low volatility. ACCs show high concentrations only in the Amazon, Central Africa and Western Europe (Fig. S3) where the total nucleation rate is dominated by pure organic nucleation (Figs. S6 and S7). Furthermore, in these regions, there is the largest difference in ACCs concentration between PD and PI experiments (Fig. S3). Consequently, the most significant reductions in  $ERF_{aci}$  are in the Amazon, central Africa, Australia, and Southeast Asia (Fig. 6b), as well as the marine low-cloud regions to the west of these areas.

295

300

## 5 Summary and discussion

305

New particle formation (NPF) is widely recognized as an important source of atmospheric particles that significantly influence the Earth's climate. In the present work, the contribution of highly oxygenated organic molecules (HOMs) to cloud condensation nuclei (CCN) burden via organic nucleation is quantified in both present-day (PD) and preindustrial (PI) environments using a chemistry-climate model (Shao et al., 2024). The reduction in effective radiative forcing due to aerosol-cloud interactions ( $ERF_{aci}$ ) caused by adding organic NPF mechanisms is also assessed.

310

After incorporating organic NPF scheme with state-of-the-art chemical mechanisms for biogenic HOMs into CAM6-Chem, the simulated CCN numbers agree better with measurements across different backgrounds (Fig. 1). Globally, the inclusion of organic-related NPF processes results in a 39% increase in CCN burden in the PI experiment and an 18% increase in the PD experiment. Similarly, cloud droplet number concentration (CDNC) at the top of low clouds in the Inorg\_Org simulation rises by 12% in the PI experiment but only by 7% in the PD experiment. The greater enhancement of CCN burden in the PI experiment is primarily driven by organic condensational growth on sub-20 nm particles, rather than organic nucleation. The main reason is that sulfuric acid ( $H_2SO_4$ ) concentrations are significantly higher in the PD environment (Fig. S2), leading to higher heteromolecular nucleation rates of sulfuric acid and organics ( $J_{SA-Org}$ ), which is the largest contributors to organic nucleation in most regions. In contrast, HOM concentrations are higher in the PI atmosphere (Fig. S3) leading to a much greater condensation of organics on sub-20 nm particles in PI experiments

320



325 The larger increase in both CCN and CDNC in the PI environment directly leads to an increased aerosol indirect effect in the PI, which is the baseline for calculating  $ERF_{aci}$  in the global model, thereby decreasing the cooling effect of  $ERF_{aci}$  ( $\sim 0.42 \text{ W m}^{-2}$ , corresponding to 16% of its original magnitude) (Fig. 9). The reduction in the magnitude of  $ERF_{aci}$  is primarily concentrated in boreal forests and low latitudes (Amazon, central Africa, and Southeast China), consistent with the higher increase in CCN and cloud droplet numbers in the PI atmosphere of those regions.

330 Although we utilized explicit chemical reactions to replace the traditional fixed yield method for simulating biogenic HOMs concentrations, further studies are needed to better align simulated HOM concentrations with widespread measurements. For instance, the autoxidation reaction step, which likely affects the volatility of the final products and their contribution to organic nucleation, has not yet been conclusively determined in chamber experiments (Roldin et al., 2019; Weber et al., 2020; Berndt et al., 2018). Also, the mechanisms used in this study cannot yet capture all variations in observed NPF events (Shao et al., 2024), especially in polluted environments. More lab-based studies are needed to examine the chemical reactions of anthropogenic HOMs to identify which could contribute to NPF mechanisms.

335 Despite the many uncertainties in NPF mechanisms, we present the estimated weakening of  $ERF_{aci}$  caused by incorporating state-of-the-art biogenic NPF mechanisms in the global model, with a greater reduction than estimated in previous studies. This finding implies that the climate is more sensitive to biogenic emissions and less sensitive to anthropogenic emissions than previously thought. This insight could be broadly applicable in the context of future carbon neutrality when anthropogenic gases and aerosols will decrease, but biogenic emissions will likely increase..

**Competing interests.** At least one of the (co-)authors is a member of the editorial board of Atmospheric Chemistry and Physics.

345 **Acknowledgments.** This work is supported by the National Natural Science Foundation of China (grant nos. 41925023, U2342223, and 91744208), and the Fundamental Research Funds for the Central Universities - CEMAC “GeoX” Interdisciplinary Program (2024ZD05) by the Frontiers Science Center for Critical Earth Material Cycling, Nanjing University. We greatly thank the High Performance Computing Center (HPCC) of Nanjing University for providing the computational resources used in this work. We thank all the scientists, software engineers, and administrators, who contributed to the development of CESM2.

350 **Author contributions.** MW and XD designed the study. XS performed the data analysis, produced the figures, and wrote the manuscript draft. LR and MY collected the dataset. YL, SA, WS, HW, JW, XZ and KS contributed to the analysis methods. DJ provided the model. All the authors contributed to discussion, writing, and editing of the manuscript.

355





## References

- Albrecht, B. A.: Aerosols, Cloud Microphysics, and Fractional Cloudiness, *Science*, 245, 1227-1230, doi:10.1126/science.245.4923.1227, 1989.
- 360 Berndt, T., Mentler, B., Scholz, W., Fischer, L., Herrmann, H., Kulmala, M., and Hansel, A.: Accretion Product Formation from Ozonolysis and OH Radical Reaction of  $\alpha$ -Pinene: Mechanistic Insight and the Influence of Isoprene and Ethylene, *Environ. Sci. Technol.*, 52, 11069-11077, 10.1021/acs.est.8b02210, 2018.
- Bianchi, F., Kurten, T., Riva, M., Mohr, C., Rissanen, M. P., Roldin, P., Berndt, T., Crouse, J. D., Wennberg, P. O., Mentel, T. F., Wildt, J., Junninen, H., Jokinen, T., Kulmala, M., Worsnop, D. R., Thornton, J. A., Donahue, N., Kjaergaard, H. G., and Ehn, M.: Highly Oxygenated Organic Molecules (HOM) from Gas-Phase Autoxidation Involving Peroxy Radicals: A Key Contributor to Atmospheric
- 365 Aerosol, *Chem. Rev.*, 119, 3472-3509, 10.1021/acs.chemrev.8b00395, 2019.
- Bodhaine, B. A.: Aerosol measurements at four background sites, *J. Geophys. Res.-Oceans*, 88, 10753-10768, <https://doi.org/10.1029/JC088iC15p10753>, 1983.
- Carslaw, K. S., Lee, L. A., Reddington, C. L., Pringle, K. J., Rap, A., Forster, P. M., Mann, G. W., Spracklen, D. V., Woodhouse, M. T., Regayre, L. A., and Pierce, J. R.: Large contribution of natural aerosols to uncertainty in indirect forcing, *Nature*, 503, 67-71, 10.1038/nature12674, 2013.
- 370 Dunne, E. M., Gordon, H., Kurten, A., Almeida, J., Duplissy, J., Williamson, C., Ortega, I. K., Pringle, K. J., Adamov, A., Baltensperger, U., Barmet, P., Benduhn, F., Bianchi, F., Breitenlechner, M., Clarke, A., Curtius, J., Dommen, J., Donahue, N. M., Ehrhart, S., Flagan, R. C., Franchin, A., Guida, R., Hakala, J., Hansel, A., Heinritzi, M., Jokinen, T., Kangasluoma, J., Kirkby, J., Kulmala, M., Kupc, A., Lawler, M. J., Lehtipalo, K., Makhmutov, V., Mann, G., Mathot, S., Merikanto, J., Miettinen, P., Nenes, A., Onnela, A., Rap, A., Reddington, C.
- 375 L. S., Riccobono, F., Richards, N. A. D., Rissanen, M. P., Rondo, L., Sarnela, N., Schobesberger, S., Sengupta, K., Simon, M., Sipilaa, M., Smith, J. N., Stozkhov, Y., Tome, A., Trostl, J., Wagner, P. E., Wimmer, D., Winkler, P. M., Worsnop, D. R., and Carslaw, K. S.: Global atmospheric particle formation from CERN CLOUD measurements, *Science*, 354, 1119-1124, 10.1126/science.aaf2649, 2016.
- Ehn, M., Thornton, J. A., Kleist, E., Sipila, M., Junninen, H., Pullinen, I., Springer, M., Rubach, F., Tillmann, R., Lee, B., Lopez-Hilfiker, F., Andres, S., Acir, I. H., Rissanen, M., Jokinen, T., Schobesberger, S., Kangasluoma, J., Kontkanen, J., Nieminen, T., Kurten, T.,
- 380 Nielsen, L. B., Jorgensen, S., Kjaergaard, H. G., Canagaratna, M., Dal Maso, M., Berndt, T., Petaja, T., Wahner, A., Kerminen, V. M., Kulmala, M., Worsnop, D. R., Wildt, J., and Mentel, T. F.: A large source of low-volatility secondary organic aerosol, *Nature*, 506, 476-+, 10.1038/nature13032, 2014.
- Emmons, L. K., Schwantes, R. H., Orlando, J. J., Tyndall, G., Kinnison, D., Lamarque, J. F., Marsh, D., Mills, M. J., Tilmes, S., Bardeen, C., Buchholz, R. R., Conley, A., Gattelman, A., Garcia, R., Simpson, I., Blake, D. R., Meinardi, S., and Pétron, G.: The Chemistry Mechanism in the Community Earth System Model Version 2 (CESM2), *J. Adv. Model. Earth Sy.*, 12, 10.1029/2019ms001882, 2020.
- 385 Ghan, S. J.: Technical Note: Estimating aerosol effects on cloud radiative forcing, *Atmos. Chem. Phys.*, 13, 9971-9974, 10.5194/acp-13-9971-2013, 2013.
- Gordon, H., Kirkby, J., Baltensperger, U., Bianchi, F., Breitenlechner, M., Curtius, J., Dias, A., Dommen, J., Donahue, N. M., Dunne, E. M., Duplissy, J., Ehrhart, S., Flagan, R. C., Frege, C., Fuchs, C., Hansel, A., Hoyle, C. R., Kulmala, M., Kurten, A., Lehtipalo, K., Makhmutov, V., Molteni, U., Rissanen, M. P., Stozkhov, Y., Trostl, J., Tsagkogeorgas, G., Wagner, R., Williamson, C., Wimmer, D., Winkler, P. M., Yan, C., and Carslaw, K. S.: Causes and importance of new particle formation in the present-day and preindustrial atmospheres, *J. Geophys. Res.-Atmos.*, 122, 8739-8760, 10.1002/2017jd026844, 2017.
- 390 Gordon, H., Sengupta, K., Rap, A., Duplissy, J., Frege, C., Williamson, C., Heinritzi, M., Simon, M., Yan, C., Almeida, J., Trostl, J., Nieminen, T., Ortega, I. K., Wagner, R., Dunne, E. M., Adamov, A., Amorim, A., Bernhammer, A. K., Bianchi, F., Breitenlechner, M., Brilke, S., Chen, X. M., Craven, J. S., Dias, A., Ehrhart, S., Fischer, L., Flagan, R. C., Franchin, A., Fuchs, C., Guida, R., Hakala, J., Hoyle, C. R., Jokinen, T., Junninen, H., Kangasluoma, J., Kim, J., Kirkby, J., Krapf, M., Kurten, A., Laaksonen, A., Lehtipalo, K., Makhmutov, V., Mathot, S., Molteni, U., Monks, S. A., Onnela, A., Perakyla, O., Piel, F., Petaja, T., Praplanh, A. P., Pringle, K. J., Richards, N. A. D., Rissanen, M. P., Rondo, L., Sarnela, N., Schobesberger, S., Scott, C. E., Seinfeldo, J. H., Sharma, S., Sipilaa, M., Steiner, G., Stozkhov, Y., Stratmann, F., Tome, A., Virtanen, A., Vogel, A. L., Wagner, A. C., Wagner, P. E., Weingartner, E., Wimmer, D., Winkler, P. M., Ye, P. L., Zhang, X., Hansel, A., Dommen, J., Donahue, N. M., Worsnop, D. R., Baltensperger, U., Kulmala, M., Curtius, J., and Carslaw, K. S.: Reduced anthropogenic aerosol radiative forcing caused by biogenic new particle formation, *P. Natl. Acad. Sci. USA*, 113, 12053-12058, 10.1073/pnas.1602360113, 2016.
- 400 Guenther, A. B., Jiang, X., Heald, C. L., Sakulyanontvittaya, T., Duhl, T., Emmons, L. K., and Wang, X.: The Model of Emissions of Gases and Aerosols from Nature version 2.1 (MEGAN2.1): an extended and updated framework for modeling biogenic emissions, *Geosci. Model Dev.*, 5, 1471-1492, 10.5194/gmd-5-1471-2012, 2012.
- 405 Heinritzi, M., Dada, L., Simon, M., Stolzenburg, D., Wagner, A. C., Fischer, L., Ahonen, L. R., Amanatidis, S., Baalbaki, R., Baccharini, A., Bauer, P. S., Baumgartner, B., Bianchi, F., Brilke, S., Chen, D., Chiu, R., Dias, A., Dommen, J., Duplissy, J., Finkenzeller, H., Frege, C., Fuchs, C., Garmash, O., Gordon, H., Granzin, M., El Haddad, I., He, X., Helm, J., Hofbauer, V., Hoyle, C. R., Kangasluoma, J., Keber, T., Kim, C., Kürten, A., Lamkaddam, H., Laurila, T. M., Lampilahti, J., Lee, C. P., Lehtipalo, K., Leiminger, M., Mai, H., Makhmutov, V., Manninen, H. E., Marten, R., Mathot, S., Mauldin, R. L., Mentler, B., Molteni, U., Müller, T., Nie, W., Nieminen, T., Onnela, A., Partoll, E., Passananti, M., Petäjä, T., Pfeifer, J., Pospisilova, V., Quéléver, L. L. J., Rissanen, M. P., Rose, C., Schobesberger, S., Scholz, W.,





- 415 Scholze, K., Sipilä, M., Steiner, G., Stozhkov, Y., Tauber, C., Tham, Y. J., Vazquez-Pufleau, M., Virtanen, A., Vogel, A. L., Volkamer, R., Wagner, R., Wang, M., Weitz, L., Wimmer, D., Xiao, M., Yan, C., Ye, P., Zha, Q., Zhou, X., Amorim, A., Baltensperger, U., Hansel, A., Kulmala, M., Tomé, A., Winkler, P. M., Worsnop, D. R., Donahue, N. M., Kirkby, J., and Curtius, J.: Molecular understanding of the suppression of new-particle formation by isoprene, *Atmos. Chem. Phys.*, 20, 11809-11821, 10.5194/acp-20-11809-2020, 2020.
- Hoesly, R. M., Smith, S. J., Feng, L., Klimont, Z., Janssens-Maenhout, G., Pitkanen, T., Seibert, J. J., Vu, L., Andres, R. J., Bolt, R. M., Bond, T. C., Dawidowski, L., Kholod, N., Kurokawa, J. I., Li, M., Liu, L., Lu, Z., Moura, M. C. P., O'Rourke, P. R., and Zhang, Q.: Historical (1750–2014) anthropogenic emissions of reactive gases and aerosols from the Community Emissions Data System (CEDS), *Geosci. Model Dev.*, 11, 369-408, 10.5194/gmd-11-369-2018, 2018.
- 420 Jefferson, A.: Empirical estimates of CCN from aerosol optical properties at four remote sites, *Atmos. Chem. Phys.*, 10, 6855-6861, 10.5194/acp-10-6855-2010, 2010.
- Jokinen, T., Berndt, T., Makkonen, R., Kerminen, V. M., Junninen, H., Paasonen, P., Stratmann, F., Herrmann, H., Guenther, A. B., Worsnop, D. R., Kulmala, M., Ehn, M., and Sipilä, M.: Production of extremely low volatile organic compounds from biogenic emissions: Measured yields and atmospheric implications, *P. Natl. Acad. Sci. USA*, 112, 7123-7128, 10.1073/pnas.1423977112, 2015.
- 425 Kazil, J., Stier, P., Zhang, K., Quaas, J., Kinne, S., O'Donnell, D., Rast, S., Esch, M., Ferrachat, S., Lohmann, U., and Feichter, J.: Aerosol nucleation and its role for clouds and Earth's radiative forcing in the aerosol-climate model ECHAM5-HAM, *Atmos. Chem. Phys.*, 10, 10733-10752, 10.5194/acp-10-10733-2010, 2010.
- Kerminen, V. M. and Kulmala, M.: Analytical formulae connecting the "real" and the "apparent" nucleation rate and the nuclei number concentration for atmospheric nucleation events, *J. Atmos. Sci.*, 33, 609-622, 10.1016/s0021-8502(01)00194-x, 2002.
- 430 Kirkby, J., Duplissy, J., Sengupta, K., Frege, C., Gordon, H., Williamson, C., Heinritzi, M., Simon, M., Yan, C., Almeida, J., Trostl, J., Nieminen, T., Ortega, I. K., Wagner, R., Adamov, A., Amorim, A., Bernhammer, A. K., Bianchi, F., Breitenlechner, M., Brilke, S., Chen, X. M., Craven, J., Dias, A., Ehrhart, S., Flagan, R. C., Franchin, A., Fuchs, C., Guida, R., Hakala, J., Hoyle, C. R., Jokinen, T., Junninen, H., Kangasluoma, J., Kim, J., Krapf, M., Kurten, A., Laaksonen, A., Lehtipalo, K., Makhmutov, V., Mathot, S., Molteni, U., Onnela, A., Perakyla, O., Piel, F., Petaja, T., Praplan, A. P., Pringle, K., Rap, A., Richards, N. A. D., Riipinen, I., Rissanen, M. P., Rondo, L., Sarnela, N., Schobesberger, S., Scott, C. E., Seinfeld, J. H., Sipilä, M., Steiner, G., Stozhkov, Y., Stratmann, F., Tome, A., Virtanen, A., Vogel, A. L., Wagner, A. C., Wagner, P. E., Weingartner, E., Wimmer, D., Winkler, P. M., Ye, P. L., Zhang, X., Hansel, A., Dommen, J., Donahue, N. M., Worsnop, D. R., Baltensperger, U., Kulmala, M., Carslaw, K. S., and Curtius, J.: Ion-induced nucleation of pure biogenic particles, *Nature*, 533, 521-+, 10.1038/nature17953, 2016.
- 435 Kooperman, G. J., Pritchard, M. S., Ghan, S. J., Wang, M., Somerville, R. C. J., and Russell, L. M.: Constraining the influence of natural variability to improve estimates of global aerosol indirect effects in a nudged version of the Community Atmosphere Model 5, *J. Geophys. Res.-Atmos.*, 117, 10.1029/2012jd018588, 2012.
- Kulmala, M., Lehtinen, K. E. J., and Laaksonen, A.: Cluster activation theory as an explanation of the linear dependence between formation rate of 3nm particles and sulphuric acid concentration, *Atmos. Chem. Phys.*, 6, 787-793, 10.5194/acp-6-787-2006, 2006.
- 445 Lee, S.-H., Gordon, H., Yu, H., Lehtipalo, K., Haley, R., Li, Y., and Zhang, R.: New Particle Formation in the Atmosphere: From Molecular Clusters to Global Climate, *J. Geophys. Res. Atmos.*, 124, 7098-7146, <https://doi.org/10.1029/2018JD029356>, 2019.
- Li, M., Liu, H., Geng, G., Hong, C., Liu, F., Song, Y., Tong, D., Zheng, B., Cui, H., Man, H., Zhang, Q., and He, K.: Anthropogenic emission inventories in China: a review, *National Science Review*, 4, 834-866, 10.1093/nsr/nwx150, 2017.
- Liu, X., Ma, P. L., Wang, H., Tilmes, S., Singh, B., Easter, R. C., Ghan, S. J., and Rasch, P. J.: Description and evaluation of a new four-mode version of the Modal Aerosol Module (MAM4) within version 5.3 of the Community Atmosphere Model, *Geosci. Model Dev.*, 9, 505-522, 10.5194/gmd-9-505-2016, 2016.
- 450 Merikanto, J., Napari, I., Vehkamäki, H., Anttila, T., and Kulmala, M.: New parameterization of sulfuric acid-ammonia-water ternary nucleation rates at tropospheric conditions, *J. Geophys. Res.-Atmos.*, 112, 10.1029/2006jd007977, 2007.
- Merikanto, J., Spracklen, D. V., Mann, G. W., Pickering, S. J., and Carslaw, K. S.: Impact of nucleation on global CCN, *Atmos. Chem. Phys.*, 9, 8601-8616, 10.5194/acp-9-8601-2009, 2009.
- 455 O'Neill, B. C., Kriegler, E., Ebi, K. L., Kemp-Benedict, E., Riahi, K., Rothman, D. S., van Ruijven, B. J., van Vuuren, D. P., Birkmann, J., Kok, K., Levy, M., and Solecki, W.: The roads ahead: Narratives for shared socioeconomic pathways describing world futures in the 21st century, *Global Environ. Change*, 42, 169-180, <https://doi.org/10.1016/j.gloenvcha.2015.01.004>, 2017.
- Peace, A. H., Carslaw, K. S., Lee, L. A., Regayre, L. A., Booth, B. B. B., Johnson, J. S., and Bernie, D.: Effect of aerosol radiative forcing uncertainty on projected exceedance year of a 1.5 °C global temperature rise, *Environ. Res. Lett.*, 15, 0940a0946, 10.1088/1748-9326/aba20c, 2020.
- 460 Rap, A., Scott, C. E., Spracklen, D. V., Bellouin, N., Forster, P. M., Carslaw, K. S., Schmidt, A., and Mann, G.: Natural aerosol direct and indirect radiative effects, *Geophys. Res. Lett.*, 40, 3297-3301, <https://doi.org/10.1002/grl.50441>, 2013.
- Reddington, C. L., Carslaw, K. S., Stier, P., Schutgens, N., Coe, H., Liu, D., Allan, J., Browse, J., Pringle, K. J., Lee, L. A., Yoshioka, M., Johnson, J. S., Regayre, L. A., Spracklen, D. V., Mann, G. W., Clarke, A., Hermann, M., Henning, S., Wex, H., Kristensen, T. B., Leaitch, W. R., Pöschl, U., Rose, D., Andreae, M. O., Schmale, J., Kondo, Y., Oshima, N., Schwarz, J. P., Nenes, A., Anderson, B., Roberts, G. C., Snider, J. R., Leck, C., Quinn, P. K., Chi, X., Ding, A., Jimenez, J. L., and Zhang, Q.: The Global Aerosol Synthesis and Science Project



- (GASSP): Measurements and Modeling to Reduce Uncertainty, *Bull. Amer. Meteor. Soc.*, 98, 1857-1877, 10.1175/bams-d-15-00317.1, 2017.
- 470 Riccobono, F., Schobesberger, S., Scott, C. E., Dommen, J., Ortega, I. K., Rondo, L., Almeida, J., Amorim, A., Bianchi, F., Breitenlechner, M., David, A., Downard, A., Dunne, E. M., Duplissy, J., Ehrhart, S., Flagan, R. C., Franchin, A., Hansel, A., Junninen, H., Kajos, M., Keskinen, H., Kupc, A., Kurten, A., Kvashin, A. N., Laaksonen, A., Lehtipalo, K., Makhmutov, V., Mathot, S., Nieminen, T., Onnela, A., Petaja, T., Praplan, A. P., Santos, F. D., Schallhart, S., Seinfeld, J. H., Sipila, M., Spracklen, D. V., Stozhkov, Y., Stratmann, F., Tome, A., Tsagkogeorgas, G., Vaattovaara, P., Viisanen, Y., Virtala, A., Wagner, P. E., Weingartner, E., Wex, H., Wimmer, D., Carslaw, K. S., Curtius, J., Donahue, N. M., Kirkby, J., Kulmala, M., Worsnop, D. R., and Baltensperger, U.: Oxidation Products of Biogenic Emissions Contribute to Nucleation of Atmospheric Particles, *Science*, 344, 717-721, 10.1126/science.1243527, 2014.
- 475 Roldin, P., Ehn, M., Kurtén, T., Olenius, T., Rissanen, M. P., Sarnela, N., Elm, J., Rantala, P., Hao, L., Hyttinen, N., Heikkinen, L., Worsnop, D. R., Pichelstorfer, L., Xavier, C., Clusius, P., Öström, E., Petäjä, T., Kulmala, M., Vehkamäki, H., Virtanen, A., Riipinen, I., and Boy, M.: The role of highly oxygenated organic molecules in the Boreal aerosol-cloud-climate system, *Nat. Commun.*, 10, 4370, 10.1038/s41467-019-12338-8, 2019.
- 480 Rosenfeld, D. and Lensky, I. M.: Satellite-Based Insights into Precipitation Formation Processes in Continental and Maritime Convective Clouds, *Bull. Amer. Meteorol. Soc.*, 79, 2457-2476, [https://doi.org/10.1175/1520-0477\(1998\)079<2457:SBIIPF>2.0.CO;2](https://doi.org/10.1175/1520-0477(1998)079<2457:SBIIPF>2.0.CO;2), 1998.
- Rosenfeld, D. and Woodley, W. L.: Deep convective clouds with sustained supercooled liquid water down to -37.5 °C, *Nature*, 405, 440-442, 10.1038/35013030, 2000.
- 485 Schwantes, R. H., Emmons, L. K., Orlando, J. J., Barth, M. C., Tyndall, G. S., Hall, S. R., Ullmann, K., St. Clair, J. M., Blake, D. R., Wisthaler, A., and Bui, T. P. V.: Comprehensive isoprene and terpene gas-phase chemistry improves simulated surface ozone in the southeastern US, *Atmos. Chem. Phys.*, 20, 3739-3776, 10.5194/acp-20-3739-2020, 2020.
- Seinfeld, J. H., Bretherton, C., Carslaw, K. S., Coe, H., DeMott, P. J., Dunlea, E. J., Feingold, G., Ghan, S., Guenther, A. B., Kahn, R., Kraucunas, I., Kreidenweis, S. M., Molina, M. J., Nenes, A., Penner, J. E., Prather, K. A., Ramanathan, V., Ramaswamy, V., Rasch, P. J., Ravishankara, A. R., Rosenfeld, D., Stephens, G., and Wood, R.: Improving our fundamental understanding of the role of aerosol-cloud interactions in the climate system, *P. Natl. Acad. Sci. USA*, 113, 5781-5790, doi:10.1073/pnas.1514043113, 2016.
- 490 Shao, X., Wang, M., Dong, X., Liu, Y., Shen, W., Arnold, S. R., Regayre, L. A., Andreae, M. O., Pöhlker, M. L., Jo, D. S., Yue, M., and Carslaw, K. S.: Global modeling of aerosol nucleation with a semi-explicit chemical mechanism for highly oxygenated organic molecules (HOMs), *Atmos. Chem. Phys.*, 24, 11365-11389, 10.5194/acp-24-11365-2024, 2024.
- Sihto, S. L., Kulmala, M., Kerminen, V. M., Dal Maso, M., Petaja, T., Riipinen, I., Korhonen, H., Arnold, F., Janson, R., Boy, M., Laaksonen, A., and Lehtinen, K. E. J.: Atmospheric sulphuric acid and aerosol formation: implications from atmospheric measurements for nucleation and early growth mechanisms, *Atmos. Chem. Phys.*, 6, 4079-4091, 10.5194/acp-6-4079-2006, 2006.
- 500 Spracklen, D. V., Carslaw, K. S., Kulmala, M., Kerminen, V. M., Sihto, S. L., Riipinen, I., Merikanto, J., Mann, G. W., Chipperfield, M. P., Wiedensohler, A., Birmili, W., and Lihavainen, H.: Contribution of particle formation to global cloud condensation nuclei concentrations, *Geophysical Research Letters*, 35, 10.1029/2007gl033038, 2008.
- Thanh, N. T. K., Maclean, N., and Mahiddine, S.: Mechanisms of Nucleation and Growth of Nanoparticles in Solution, *Chem. Rev.*, 114, 7610-7630, 10.1021/cr400544s, 2014.
- Twomey, S.: The Influence of Pollution on the Shortwave Albedo of Clouds, *J. Atmos. Sci.*, 34, 1149-1152, [https://doi.org/10.1175/1520-0469\(1977\)034<1149:TIOPOT>2.0.CO;2](https://doi.org/10.1175/1520-0469(1977)034<1149:TIOPOT>2.0.CO;2), 1977.
- 505 Uin, J., Aiken, A. C., Dubey, M. K., Kuang, C., Pekour, M., Salwen, C., Sedlacek, A. J., Senum, G., Smith, S., Wang, J., Watson, T. B., and Springston, S. R.: Atmospheric Radiation Measurement (ARM) Aerosol Observing Systems (AOS) for Surface-Based In Situ Atmospheric Aerosol and Trace Gas Measurements, *J. Atmos. Ocean. Tech.*, 36, 2429-2447, <https://doi.org/10.1175/JTECH-D-19-0077.1>, 2019.
- van Marle, M. J. E., Kloster, S., Magi, B. I., Marlon, J. R., Daniau, A. L., Field, R. D., Arneth, A., Forrest, M., Hantson, S., Kehrwald, N. M., Knorr, W., Lasslop, G., Li, F., Mangeon, S., Yue, C., Kaiser, J. W., and van der Werf, G. R.: Historic global biomass burning emissions for CMIP6 (BB4CMIP) based on merging satellite observations with proxies and fire models (1750–2015), *Geosci. Model Dev.*, 10, 3329-3357, 10.5194/gmd-10-3329-2017, 2017.
- 510 Vehkamäki, H., Kulmala, M., Napari, I., Lehtinen, K. E. J., Timmreck, C., Noppel, M., and Laaksonen, A.: An improved parameterization for sulfuric acid-water nucleation rates for tropospheric and stratospheric conditions, *J. Geophys. Res.-Atmos.*, 107, 10.1029/2002jd002184, 2002.
- 515 Wang, J., Wood, R., Jensen, M. P., Chiu, J. C., Liu, Y., Lamer, K., Desai, N., Giangrande, S. E., Knopf, D. A., Kollias, P., Laskin, A., Liu, X., Lu, C., Mechem, D., Mei, F., Starzec, M., Tomlinson, J., Wang, Y., Yum, S. S., Zheng, G., Aiken, A. C., Azevedo, E. B., Blanchard, Y., China, S., Dong, X., Gallo, F., Gao, S., Ghate, V. P., Glienke, S., Goldberger, L., Hardin, J. C., Kuang, C., Luke, E. P., Matthews, A. A., Miller, M. A., Moffet, R., Pekour, M., Schmid, B., Sedlacek, A. J., Shaw, R. A., Shilling, J. E., Sullivan, A., Suski, K., Veghte, D. P., Weber, R., Wyant, M., Yeom, J., Zawadowicz, M., and Zhang, Z.: Aerosol and Cloud Experiments in the Eastern North Atlantic (ACE-ENA), *Bull. Amer. Meteorol. Soc.*, 103, E619-E641, <https://doi.org/10.1175/BAMS-D-19-0220.1>, 2022.
- 520 Wang, M. and Penner, J. E.: Aerosol indirect forcing in a global model with particle nucleation, *Atmos. Chem. Phys.*, 9, 239-260, 10.5194/acp-9-239-2009, 2009.



- 525 Wang, X., Gordon, H., Grosvenor, D. P., Andreae, M. O., and Carslaw, K. S.: Contribution of regional aerosol nucleation to low-level CCN in an Amazonian deep convective environment: results from a regionally nested global model, *Atmospheric Chemistry and Physics*, 23, 4431-4461, 10.5194/acp-23-4431-2023, 2023.
- Watson-Parris, D. and Smith, C. J.: Large uncertainty in future warming due to aerosol forcing, *Nat. Clim. Chang.*, 12, 1111-1113, 10.1038/s41558-022-01516-0, 2022.
- 530 Weber, J., Archer-Nicholls, S., Griffiths, P., Berndt, T., Jenkin, M., Gordon, H., Knote, C., and Archibald, A. T.: CRI-HOM: A novel chemical mechanism for simulating highly oxygenated organic molecules (HOMs) in global chemistry–aerosol–climate models, *Atmos. Chem. Phys.*, 20, 10889-10910, 10.5194/acp-20-10889-2020, 2020.
- Williamson, C. J., Kupc, A., Axisa, D., Bilsback, K. R., Bui, T., Campuzano-Jost, P., Dollner, M., Froyd, K. D., Hodshire, A. L., Jimenez, J. L., Kodros, J. K., Luo, G., Murphy, D. M., Nault, B. A., Ray, E. A., Weinzierl, B., Wilson, J. C., Yu, F., Yu, P., Pierce, J. R., and Brock, C. A.: A large source of cloud condensation nuclei from new particle formation in the tropics, *Nature*, 574, 399-403, 10.1038/s41586-019-1638-9, 2019.
- 535 Wood, R., Wyant, M., Bretherton, C. S., Rémillard, J., Kollias, P., Fletcher, J., Stemmler, J., de Szoeko, S., Yuter, S., Miller, M., Mechem, D., Tselioudis, G., Chiu, J. C., Mann, J. A. L., O’Connor, E. J., Hogan, R. J., Dong, X., Miller, M., Ghate, V., Jefferson, A., Min, Q., Minnis, P., Palikonda, R., Albrecht, B., Luke, E., Hannay, C., and Lin, Y.: Clouds, Aerosols, and Precipitation in the Marine Boundary Layer: An Arm Mobile Facility Deployment, *Bull. Amer. Meteorol. Soc.*, 96, 419-440, <https://doi.org/10.1175/BAMS-D-13-00180.1>, 2015.
- 540 Xu, R., Thornton, J. A., Lee, B. H., Zhang, Y., Jaeglé, L., Lopez-Hilfiker, F. D., Rantala, P., and Petäjä, T.: Global simulations of monoterpene-derived peroxy radical fates and the distributions of highly oxygenated organic molecules (HOMs) and accretion products, *Atmos. Chem. Phys.*, 22, 5477-5494, 10.5194/acp-22-5477-2022, 2022a.
- Xu, R. C., Thornton, J. A., Lee, B., Zhang, Y. X., Jaegle, L., Lopez-Hilfiker, F. D., Rantala, P., and Petaja, T.: Global simulations of monoterpene-derived peroxy radical fates and the distributions of highly oxygenated organic molecules (HOMs) and accretion products, *Atmos. Chem. Phys.*, 22, 5477-5494, 10.5194/acp-22-5477-2022, 2022b.
- 545 Yu, F., Luo, G., Liu, X., Easter, R. C., Ma, X., and Ghan, S. J.: Indirect radiative forcing by ion-mediated nucleation of aerosol, *Atmos. Chem. Phys.*, 12, 11451-11463, 10.5194/acp-12-11451-2012, 2012.
- Yue, M., Dong, X., Wang, M., Emmons, L. K., Liang, Y., Tong, D., Liu, Y., and Liu, Y.: Modeling the Air Pollution and Aerosol-PBL Interactions Over China Using a Variable-Resolution Global Model, *J. Geophys. Res.-Atmos.*, 128, 10.1029/2023jd039130, 2023.
- 550 Zhao, B., Fast, J., Shrivastava, M., Donahue, N. M., Gao, Y., Shilling, J. E., Liu, Y., Zaveri, R. A., Gaudet, B., Wang, S., Wang, J., Li, Z., and Fan, J.: Formation Process of Particles and Cloud Condensation Nuclei Over the Amazon Rainforest: The Role of Local and Remote New-Particle Formation, *Geophys. Res. Lett.*, 49, e2022GL100940, <https://doi.org/10.1029/2022GL100940>, 2022.
- Zhao, B., Shrivastava, M., Donahue, N. M., Gordon, H., Schervish, M., Shilling, J. E., Zaveri, R. A., Wang, J., Andreae, M. O., Zhao, C., Gaudet, B., Liu, Y., Fan, J., and Fast, J. D.: High concentration of ultrafine particles in the Amazon free troposphere produced by organic new particle formation, *Proc Natl Acad Sci U S A*, 117, 25344-25351, 10.1073/pnas.2006716117, 2020.
- 555 Zheng, G., Sedlacek, A. J., Aiken, A. C., Feng, Y., Watson, T. B., Raveh-Rubin, S., Uin, J., Lewis, E. R., and Wang, J.: Long-range transported North American wildfire aerosols observed in marine boundary layer of eastern North Atlantic, *Environ. Int.*, 139, 105680, <https://doi.org/10.1016/j.envint.2020.105680>, 2020.
- 560 Zhu, J., Penner, J. E., Yu, F., Sillman, S., Andreae, M. O., and Coe, H.: Decrease in radiative forcing by organic aerosol nucleation, climate, and land use change, *Nat. Commun.*, 10, 423, 10.1038/s41467-019-08407-7, 2019.